Fuel economy benefits of advanced techniques for CVT actuation and control

Albers, P.H.W.M.

Award date:
2005

Fuel Economy Benefits of Advanced Techniques for CVT Actuation and Control

P.H.W.M. Albers
Report number: DCT-2005-23

Supervisor:
Prof. Dr. Ir. J.J. Kok

Coach:
Dr. P.A. Veenhuizen

Master Thesis Committee:
Prof. Dr. Ir. J.J. Kok
Dr. Ir. W.J.A.E.M. Post
Dr. Ir. B.G. Vroemen
Dr. P.A.Veenhuizen

Technische Universiteit Eindhoven, the Netherlands
Department of Mechanical Engineering
Section Control Systems Technology

Eindhoven, February 28, 2005

Summary

Modern control techniques allow drive train components to operate under more optimal operating conditions than previously possible. Powerful electric servo-motors and modern controllers are necessary for the development and refinement of automated transmissions like the Double Clutch Transmission and the Continuously Variable Transmission, in order to arrive at fuel consumption, comfort and performance levels that are expected from today's power trains.

In order to benchmark the effect of various improvement measures on fuel economy at an early stage in the development process based on above-mentioned technologies, detailed simulations can be made. This paper describes the results of a simulation study of the effects on efficiency and fuel economy of a vehicle equipped with a CVT, resulting from the introduction of the following new variator actuation and control techniques [1]:

- Replacement of the high pressure hydraulic pump by a servo-electromechanical actuation system (EMPAct) and
- introduction of variator slip control

For this study, the TNO-Advance simulation package is used, in which detailed models of all loss contributions of the CVT were implemented. The fuel economy benefit is shown to be substantial, about 6% on the NEDC cycle.

Contents

10th EAEC European Automotive Congress 2005, Belgrade

Fuel Economy Benefits of Advanced Techniques for CVT Actuation and Control

P.H.W.M. Albers*, P.A. Veenhuizen*

10th EAEC European Automotive Congress 2005, Belgrade

Abstract

Modern control techniques allow drive train components to operate under more optimal operating conditions than previously possible. Powerful electric servo-motors and modern controllers are necessary for the development and refinement of automated transmissions like the Double Clutch Transmission and the Continuously Variable Transmission, in order to arrive at fuel consumption, comfort and performance levels that are expected from today's power trains.

In order to benchmark the effect of various improvement measures on fuel economy at an early stage in the development process based on above-mentioned technologies, detailed simulations can be made. This paper describes the results of a simulation study of the effects on efficiency and fuel economy of a vehicle equipped with a CVT, resulting from the introduction of the following new variator actuation and control techniques [1]:

- Replacement of the high pressure hydraulic pump by a servo-electromechanical actuation system (EMPAct) and
- Introduction of variator slip control

For this study, the TNO-Advance simulation package is used, in which detailed models of all loss contributions of the CVT were implemented. The fuel economy benefit of the EMPAct system in comparison to the conventional CVT is shown to be substantial, about 6% on the NEDC cycle.

Keywords: continuously variable transmission, simulation, power train modeling, efficiency, CVT

---

* Technische Universiteit Eindhoven, Department of Mechanical Engineering, P.O. Box 513, 5600 MB Eindhoven, The Netherlands

1 Introduction

Since its introduction over 15 years ago, the CVT has contributed to the improvement of fuel economy of passenger cars. It gives a better fuel economy than the stepped automatic transmission (AT) due to its wider ratio coverage and its ability to shift ratio without compromising comfort. Another advantage is that it allows for the torque converter to lock up at lower vehicle speeds than when an AT is applied. Unfortunately, the metal V-belt CVT does not have a much better efficiency than the AT. An important reason for this is that it needs significantly higher hydraulic pressure for variator actuation purposes, (typically up to 50 [bar]) than an AT does, which leads to a larger oil pump drive torque. Since the oil pump usually rotates at a speed proportional to engine speed, quick ratio shifts at low engine speed dictate rather large pump displacement. For a typical CVT, rated at 200 [Nm], the pump displacement amounts to about 19 [cc/rev]. Making use of the double piston principle in combination with a two stage torque sensor, allows for a more favorable pump displacement of 11 [cc/rev] at 310 [Nm] rated torque [2].

Additionally, the power loss in the variator (defined as belt, pulleys and shaft bearings) is not small. This leads to transmission efficiencies which barely exceed 90 [%] at rated load. Under part load conditions, efficiency drops even further. This is caused by limitations in the actuation system, preventing the clamping force to drop to sufficiently low values, causing over-clamping. In order to prevent variator slip, over-clamping is applied, causing increased variator torque loss. It is mainly by these causes that the efficiency may have dropped to values below 75 [%] at 25 [%] of rated load. On various driving cycles used for fuel consumption benchmarks, a large time fraction is spent in part load conditions. Therefore, improving part load efficiency receives considerable attention. Improving efficiency at rated load will be beneficial for high torque situations like top speed, launch and fast acceleration maneuvers.

In order to reduce actuation system power consumption, Bradley and Frank [3] proposed a servo-electro hydraulic system, largely eliminating excessive oil flow. The pumps need to deliver enough flow to compensate for seal leak. A reduction of actuation power of about one order of magnitude was reported.

By using variator slip as a control variable for determining the distance between actual clamping force and the slip threshold at which the variator is irreversibly damaged, Faust et. al. [2] indicate a transmission efficiency improvement of almost 2 [%].

This paper first shows the principle of the CVT. Next, the modeling of the efficiency of the reference transmission will be presented. The most important models, describing variator torque and slip loss and pump power loss, were based on measurements on a commercially available CVT. Losses in the final drive and clutch drag losses are based on literature data. Next the transmission efficiency improvements that can be expected after replacing the hydraulic pump with a servo-electromechanical actuation system (EMPAct) and after introduction of variator slip control will be presented. Simulations will show the fuel consumption benefit of these measures.

For the EMPAct system simulations are made in Matlab/ Advance. Advance is a simulation package developed by TNO Automotive. The EMPAct system strongly reduces the power needed for clamping and shifting the variator. It avoids the situation where an engine driven pump delivers excess oil at high pressure at elevated engine speeds, thereby not only improving part load but also full load transmission efficiency. Slip control allows the variator clamping force to be set to very low values, thereby avoiding losses associated with over-clamping. Slip losses, which are usually neglected in a CVT efficiency assessment, are seen to increase somewhat when the clamping force is lowered and must therefore be taken into account. The models for the EMPAct system and the slip controller are implemented in the Advance simulation and the results are compared to the measurements.

2 Continuously Variable Transmission

Applying a Continuously Variable Transmission (CVT) in an automotive driveline has several advantages. A CVT can operate at a wider range of transmission ratios, therefore the engine can be operated more efficiently than with a stepped transmission. Also, a CVT does not abruptly change the torque level when shifting. This gives a smoother ride than a stepped transmission does. A V-belt based CVT uses a belt or a chain to transmit torque from a driving side to a driven side by means of friction. The layout of the CVT and the V-belt are shown in Fig. 1 and Fig. 2.

The variator consists of two pulleys, which are wedge shaped. Both pulley sets have a fixed and a moveable pulley, in opposite position. The movable pulleys are actuated by hydraulic pressure cylinders. By changing the axial position of the pulley sheaves the ratio of the CVT can be adjusted. The variator can cover any ratio between two extremes as shown in Fig. 1, low and overdrive.

The V-belt consists of blocks, which are held together by two rings. These rings consist of a set of bands, see Fig. 2. To achieve torque transmission, sufficiently high clamping force levels are needed to prevent slip in the variator. Because the torque level is not exactly known at all times, since no torque sensor is used due to cost and packaging considerations, a safe clamping force level based on the maximum possible load is maintained at all times. This safety level is based on the assumed maximum shock load levels from the road and the engine torque.

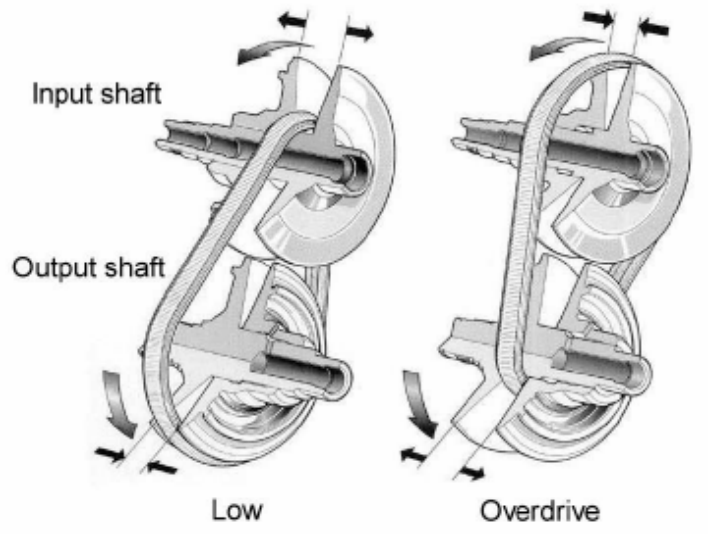

Figure 1: Low ratio and Overdrive

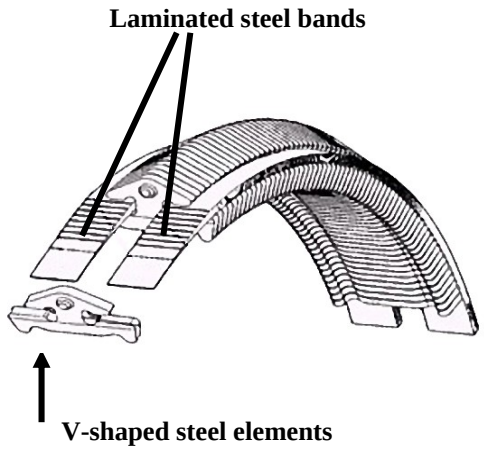

Figure 2: V-belt with steel bands

3 Reference transmission efficiency modeling

For benchmark purposes, the 2 liter class Jatco CK2, manufactured by Jatco Transtechnology Co. Ltd. is selected. This type of transmission will also be used as a carrier for the servo-electromechanical actuation system that is currently in the realization phase. The reference transmission comprises a torque converter as drive-off element, a DNR set, a hypotrochoid gear pump, a push-belt type variator, followed by the final reduction and differential gear [4]. The majority of the presented data will be limited to the over-drive ratio, since this ratio is most relevant for fuel economy evaluations.

3.1 TRANSMISSION LOSS ANALYSIS METHOD

In order to assess the efficiency improvement potential of the proposed modifications, first the power loss occurring in the reference transmission were carefully modeled. The main power losses are caused by the hydraulic pump and by the variator and were obtained by means of measurements. Losses in the final reduction were calculated by means of models obtained from literature [5]. These loss components will be treated separately in the following sections.

3.2 PUMP LOSS

One of the major loss sources within the transmission is the power absorbed in driving the hydraulic pump. This loss was measured on a spin loss test rig. This test rig allows driving the transmission with unloaded output. For these measurements, the clutch plates of the DNR set were removed to eliminate the torque loss due to friction between clutch plates. In order to control pump torque independent from the original transmission controller, a separate pressure control system was developed. The dependence of pump power loss on input speed (equal to engine speed), pump output pressure (equal to the clamping pressure in the secondary variator cylinder) and temperature, was measured in a wide operating range and mapped into lookup tables.

3.3 VARIATOR LOSSES

Contrary to form closed transmission components like gears, the variator not only loses power by torque loss, but also slip loss occurs. Although slip loss is generally much smaller than torque loss in a V-belt variator, it can not be neglected, since slip loss tends to increase when over clamping is reduced. Next the methods will be described by which these losses were analyzed.

Variator slip loss may be defined as follows:

$$\omega_{loss} = \omega_{pri} - \frac{\omega_{\sec}}{r_{\omega 0}} \tag{1}$$

A relative slip number sω can be defined by

$$s_{\omega} = \frac{\omega_{loss}}{\omega_{pri}} = 1 - \frac{r_{\omega}}{r_{\omega 0}}, with\ r_{\omega} = \frac{\omega_{\sec}}{\omega_{pri}} \tag{2}$$

Here $r_{\omega 0}$ is defined as the speed ratio r_{ω} at zero variator output load. Furthermore ω_{pri} and ω_{sec} are defined as the angular speed of the primary and secondary variator shaft, respectively. This definition ensures that s_{ω} equals zero at zero variator output load.

Power is transmitted by means of friction between the belt and the pulleys. The torque that is transmitted through the variator can be calculated using the force balance on a pulley, according to [6]:

$$T_{pri} = \frac{2F_s R_p \mu_{eff}(s_{\omega})}{\cos\lambda} \tag{3}$$

where T_{pri} is the torque on the primary shaft, F_s is the secondary clamping force, which is the axial force applied by the pulleys onto the belt, R_p represents the primary running radius of the belt, λ is half the pulley wedge angle and μ_{eff} is the effective traction coefficient between belt and pulley. The traction coefficient μ_{eff} is not constant but depends on the relative slip between the belt and the pulleys, defined by Eq. 2.

The relation between de traction coefficient μ_{eff} and the slip s_ω is shown for three ratios in Fig. 3 [8]. It can be seen that the slope of the curves and the maximum traction coefficients clearly depends on the ratio, but all curves show the same distinct shape. At first, for low slip values the traction coefficient increases with increasing slip, until a maximum value is reached. This region is called the microslip region. When the maximum value of the traction coefficient is reached, increasing slip will result in a slow decrease of the traction coefficient. This region is known as the macroslip region.

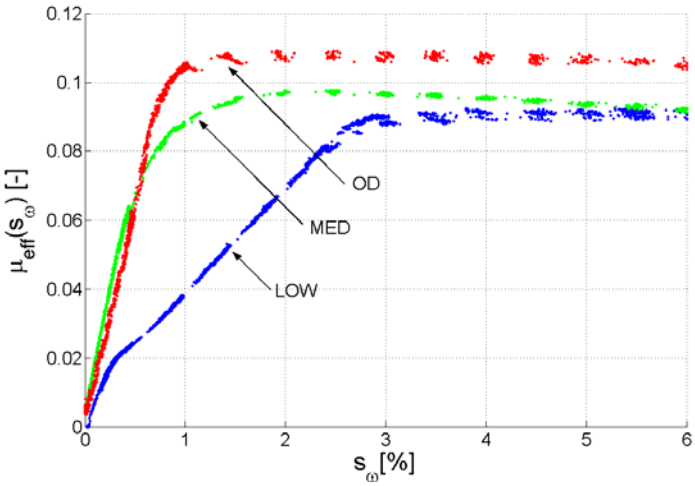

Figure 3: Traction coefficient μ_{eff} as a function of the slip s_ω measured with an input speed of 225 rad/s for ratios low (0.43), medium (1) and overdrive (2.25)

For normal operation, where only the micro-slip region is used, the dependence of torque on slip can effectively be approximated by a linear relationship. The dependence of the slope of this linear relationship on ratio and clamping force was captured in a lookup table.

Variator torque loss may be defined by:

$$T_{loss} = T_{pri} - r_{To} T_{\sec} \tag{4}$$

where T_{pri} and T_{sec} are defined as the torque on the primary and the secondary shaft respectively and r_{To} is defined as the ratio of primary torque and secondary torque at zero torque loss.

Measurements of T_{loss} have been carried out on a variator test rig. Generally, the variator torque loss is considered to be a function of four variables, i.e. secondary pressure p_{sec}, primary speed ω_{pri}, speed ratio r_ω, and input torque T_{pri}. According to measurements results shown in Fig. 4, the torque loss of the variator shows very small dependency on T_{pri}. This is in line with the literature data [7]. The solid line represents a fit of Eq. 4 to the measured data. It was therefore decided to measure torque loss under unloaded conditions (T_{sec} = 0 [Nm]) on a CK2 transmission on the same test rig that was used for pump loss determination.

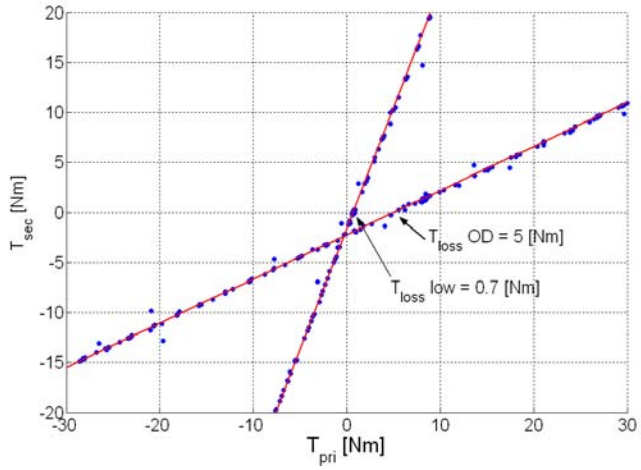

Figure 4: Variator input torque versus variator output torque at fixed secondary clamping force at low and OD ratio. The line represents a fit of Eq. 4 to the data.

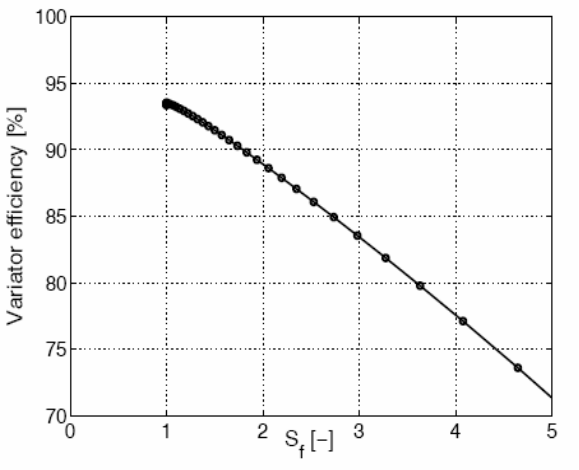

Figure 5: Variator efficiency versus safety factor S_f (over-drive, 1500 [rpm])

By removing the intermediate shaft, power loss in the final reduction was eliminated from the measurement. By switching the transmission into drive and applying torque converter lock-up and by subtracting pump torque loss from the measured data, variator torque loss as a function of input speed, ratio and clamping force could be determined over a wide operating range. A result from these measurements is shown in Fig. 5. Here, the data is used to calculate variator efficiency as a function of safety factor S_f, which is defined as the ratio of actual clamping force and the minimum clamping force, required for transfer of a specific input torque at a specific variator ratio. The graph shows that S_f must be reduced to the lowest possible value in order to obtain the best variator efficiency. Usually, lowering of the safety factor is severely limited, especially for part load conditions. Very often, the secondary or line pressure, which is directly related to secondary clamping force, cannot be lowered to values below 5-7 [bar]. This is caused by the fact that auxiliary pressures, which should not drop below 5-7 [bar], are derived from line pressure. Low safety value at low nominal torque increases the risk of variator slip caused by torque peaks originating from road irregularities. This forms another reason why safety values are seen to be considerably higher than 1 in practice.

3.4 FINAL REDUCTION LOSSES

The final drive of the CVT is similar to that found in any conventional transmission and can be modeled in a similar way. The calculations have been based on literature data [5] and references therein. Bearing losses, oil churning losses and gear meshing losses have been taken into account. During measurements it was noticed the torque losses in the final reduction depends on the applied torque to the primary shaft. This is in line with the literature data [10].

4 Reference transmission loss breakdown

The efficiency analysis mentioned in the previous sections was used to generate Fig. 6, showing the power loss breakdown of the reference transmission in overdrive at input speed of 1500 [rpm].

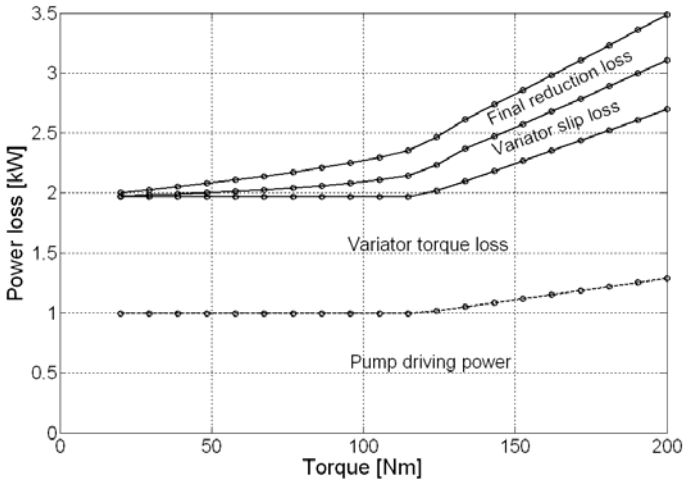

Figure 6: Loss breakdown of the reference transmission (over-drive, 1500 [rpm])

Obviously torque loss in the variator and pump loss are the most important loss sources. The change in slope occurring at about 120 [Nm] is caused by the limitation in hydraulic line pressure (equal to pressure in secondary cylinder) to drop below $p_{sec\_min} = 6.6$ [bar]. This leads to rather severe over-clamping at low torque levels, causing both pump driving loss and variator torque loss to be high.

5 Efficiency improvement options

From the previous sections it may be concluded that for the optimization of transmission efficiency by actuation and control measures, the following aspects should be taken into account:

• Over-clamping should be avoided or, equivalently, the safety factor S_f should be kept close to 1, also at low torque levels.
• In order to realize this, hydraulic limitations for lowering clamping force should be avoided
• Actuation power must be reduced

In order to realize this, a servo-electromechanical actuation system with variator slip control has been proposed, which will be described in the following sections.

5.1 VARIATOR SLIP CONTROL

As shown in Fig. 5, variator torque loss can be reduced by minimizing over-clamping. However, this increases the risk of variator slip. In order to limit variator slip as defined before, variator slip control has been proposed [8]. With this type of control, safety values very close to $S_f \cong 1$ can be realized. Road irregularities may cause short torque peaks in the drive train, causing a temporary macro-slip condition. Recent experimental results [9] have shown however, that the push-belt variator is much more robust against macro-slip than previously assumed. It will be the subject of further research to what extent this property of the push-belt variator can be used when applying slip control.

5.2 THE SERVO-ELECTROMECHANICAL ACTUATION SYSTEM

In order to assess the apparent advantages of an all-mechanic system, an electrically driven variator actuation system has been proposed by van de Meerakker et al. [1]. This system is schematically shown in Fig. 7 and is characterized by the following features:

• Both moveable sheaves are actuated by means of electric motors (Mp and Ms in Fig. 7)
• Both motors are stationary when both clamping force and variator ratio are constant. This is accomplished by applying two differential gear sets at each shaft, serving as a decoupling mechanism between the rotating transmission shafts and the transmission housing.
• By coupling two moving ring gears of the adjustment mechanisms, shifting energy can be exchanged between one movable sheave which is shifted with positive power and the other shifted with negative power.
• It is important to note that the EMPAct system calls for a novel way of estimating the clamping force, since a hydraulic pressure signal is absent. Slip control seems therefore to be a logical approach for assessing the clamping status of the variator.
• Clamping force loops are closed on the rotating shaft and not supported via the transmission housing, thereby avoiding highly loaded thrust bearings.
• A separate low pressure pump for auxiliary hydraulic functions is required.

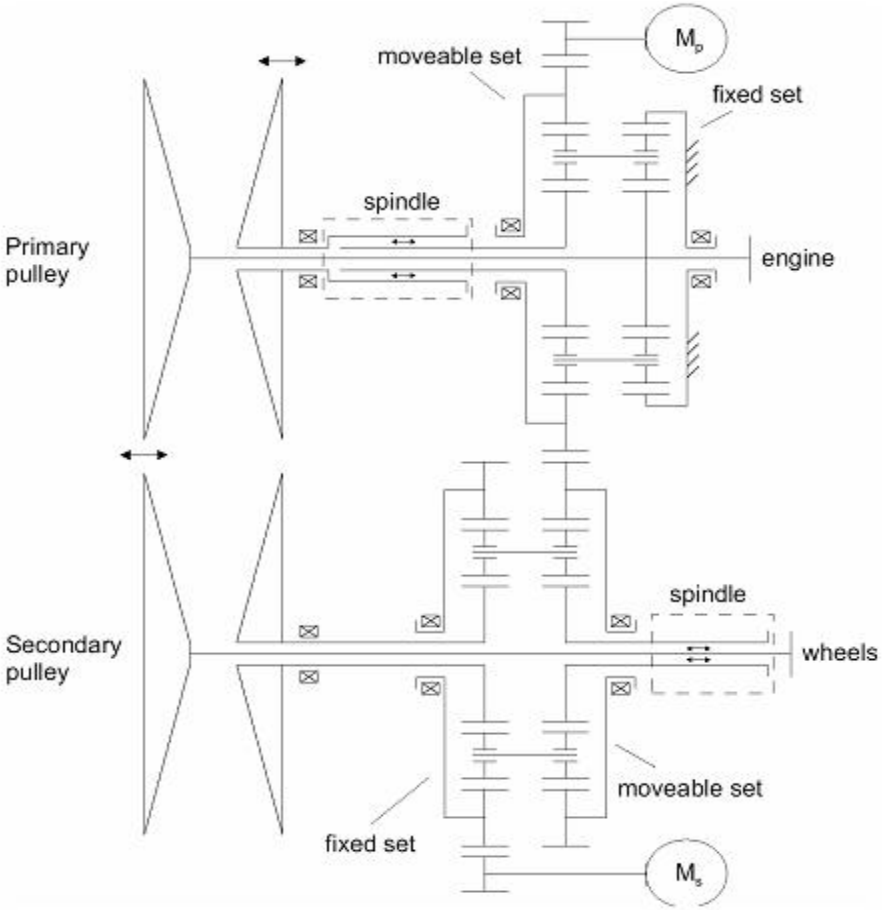

Figure 7: Schematic representation of the EMPAct system

6 Efficiency modeling for a transmission with EMPAct system

The efficiency analysis mentioned in the previous sections, was used to generate Fig. 8, showing the loss breakdown of the transmission with EMPAct system and slip control in over-drive at an input speed of 1500 [rpm]. For the torque loss calculation see also section 8. In comparison to Fig. 6 the following differences can be noted:

• The change in slope at about 120 [Nm] has disappeared. This is associated with the ability of the EMPAct system to reduce clamping force to low levels.
• Especially the power loss at part load is strongly reduced.
• Actuation power is strongly reduced.
• Part load variator torque loss is reduced considerably, which must be attributed to the reduction of over-clamping.
• Variator slip loss has increased slightly by the reduction of the safety factor to values close to 1. This is most clearly seen at high input torque levels.

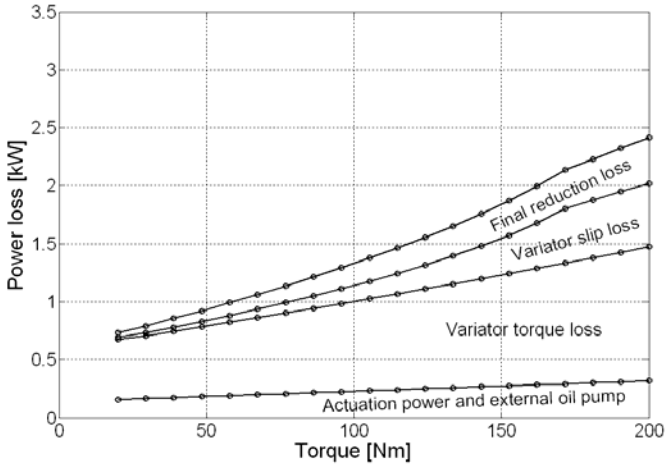

Figure 8: Loss breakdown of a transmission with EMPAct system and variator slip control (over-drive, 1500 [rpm])

In order to appreciate the contribution of the various measures to the reduction of power loss, they were analyzed separately. Table 1 defines the various improvement measures.

Table 1: Improvement measures

Variant A	Reference transmission with $S_f = 1.3$ and $p_{sec\_min} = 6.6$ [bar]
Variant B	Reference transmission with slip control, $S_f \cong 1$ and $p_{sec\_min} = 6.6$ [bar]
Variant C	Reference transmission with $S_f = 1.3$ and decreased secondary pressure $p_{sec\_min} = 1.35$ [bar]
Variant D	Slip control, $S_f \cong 1$ and $p_{sec\_min} = 1.35$[bar]
Variant E	EMPAct system, slip control $S_f \cong 1$ and $F_{sec\_min} = 1.9$ [kN]

From Fig. 9 the effects of various measures on power loss can be estimated. Curve A and curve B both have high torque losses for low input torque because of the minimum secondary pressure p_{sec_min} = 6.6 [bar]. Curve C indicates the very important effect of decreasing the clamping force boundary to a secondary pressure of p_{sec_min} = 1.35 [bar]. Curve D represents a further lowering of safety to $S_f \cong 1$, meaning that variator slip control must be applied, in order to avoid gross slip. Curve E (EMPAct system), with a minimum clamping force of 1.9 [kN] which represents a minimum line pressure of p_{sec_min} = 6.6 [bar], shows the most important loss reduction at higher torques, due to the reduction of actuation power.

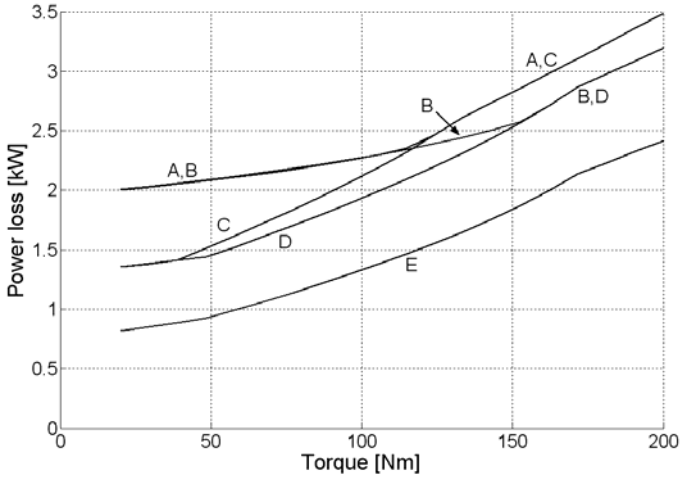

Figure 9: Loss reduction by various measures (Variants B through E) compared to the reference transmission (Variant A).

7 Measurement setup

To validate the results of the reference model a test rig is available (see Fig. 10). This test rig is designed to perform realistic drive train experiments. The rig consists of two electric Siemens motors (engine and brake), two torque sensors (Te and Ts), a Jatco CK2 CVT and a manual gearbox. The Siemens motors both include an encoder to measure the rotational speed. With the electric motors the combustion engine of a passenger car and the road load and brake torque can be simulated respectively. The torque sensors are used to measure the ingoing and outgoing torque of the CVT on the primary shaft and the drive shaft. The gearbox is used to increase the speed applied to the Siemens brake motor.

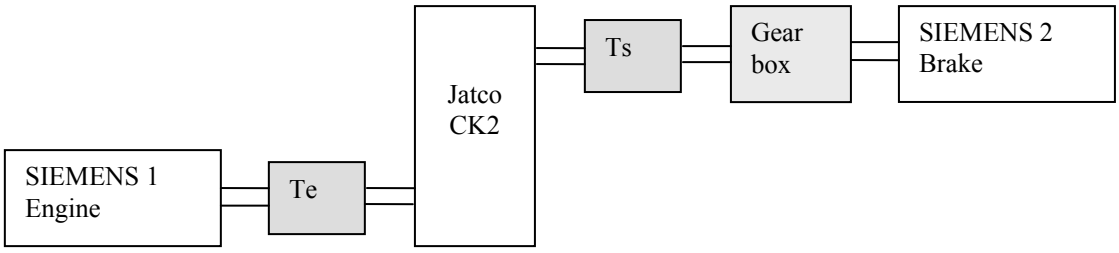

Figure 10: Overview of the test rig used for loss measurements

Normally the Jatco CK2 will be controlled by the Transmission Control Module (TCM). On this test rig no TCM is available so the clamping force to transmit engine torque has been calculated using an implemented safety 1.3 controller (Variant A from table 1) or with the slip controller (Variant B). To

simulate a driveline both electric motors should be controlled. The test rig is controlled with Matlab/ Simulink in combination with a dSpace data acquisition system.

To track a reference from a driving cycle, a driveline controller is implemented which calculates the necessary throttle position and brake torque. To obtain a stable behavior which minimizes the tracking error, a PI controller is used with anti-windup. A variogram is used to get a reference for the CVT input speed, given the vehicle speed and the throttle position. The throttle position has been calculated with an inverted engine torque map. Here the measured engine torque and engine speed result in a throttle position. With the test rig the NEDC cycle and the FTP-72 cycle are simulated. Both cycles are shown in Fig 11.

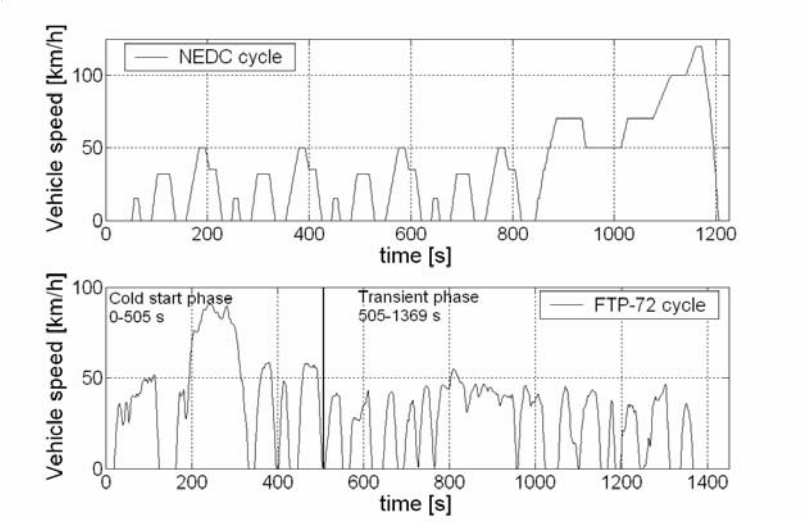

Figure 11: Speed cycles: NEDC and FTP-72

Now the results of the measurements can be compared with the results of the reference model described in chapter 3. This comparison is done in order to check the correctness of the implementation of various component loss models and also to ascertain that these models can be used also under loaded conditions. The engine speed, primary speed, secondary speed and engine torque of the measurements are the inputs for the reference model. In Fig. 12 and Fig. 13 the comparison of secondary pressure and torque loss between the measurements and the reference model (Variant A) is given. What can be noticed is the difference in secondary pressure. This difference is caused by the difference in the modeling of the torque converter. In the model only an estimated clamping force multiplier is used for take off. On the test rig the model of the torque converter has a safety factor which assures there will be enough clamping force on the secondary pulley to prevent slip. The differences in secondary pressure are shown not to have a large influence on the torque losses. Fig. 13 shows that the model predicts the torque loss accurately. Only for higher speeds and therefore higher input torque the model has some difference compared to the measurements. The most likely explanation for this discrepancy is that the final reduction exhibits more torque loss than what was calculated on the basis of models.

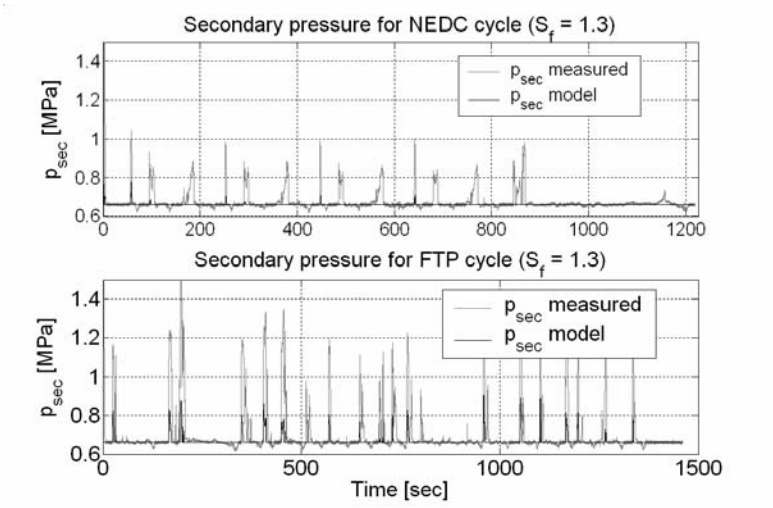

Figure 12: Secondary pressures for the NEDC and FTP-72 cycle

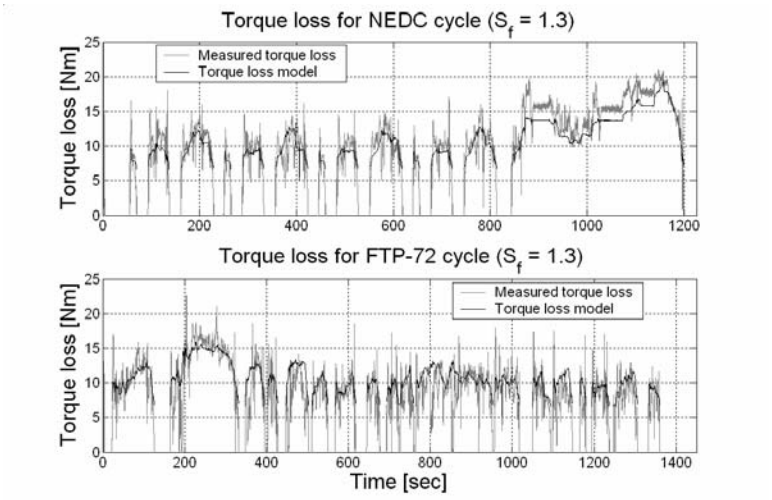

Figure 13: Torque loss for the NEDC and FTP-72 cycle

8 Modeling total EMPAct losses

For analysis, control design and testing of the electro-mechanically actuated CVT, a simulation model is built [11]. The model incorporates all major driveline components and the proposed actuation system with servomotor actuation. The clamping forces in the variator are calculated using an explicit formulation of a model based on Coulomb friction. The model also includes slip and shifting losses based on transient variator models.

For torque loss calculation due to the friction forces in the bearings, gears and spindles, Lugre friction models are incorporated in the model [11]. To calculate the power consumed by the actuation system, electromotor models and characteristics are taken into account. Also the power loss due to the external oil pump used for auxiliaries is taken into account.

9 Fuel consumption calculations with Advance

In order to assess the potential for fuel economy improvement, the data described in section 3 was used in the simulation package Advance, developed by TNO Automotive [12]. This package allows for detailed fuel consumption simulations.

With the simulation package first a comparison has been made between the results measured on the test rig and the results from Advance with the conventional CVT with control strategy S_f = 1.3 (Variant A). Both results are measured with a minimum secondary pressure of 6.6 [bar]. In Fig. 14 the torque loss and secondary pressure for the test rig and for the Advance simulation are drawn. From this figure it appears the results look sufficiently similar. The results show that the model of the torque converter in Advance can be compared to the model of the torque converter on the test rig, because now there is only a minimal difference in the secondary pressure between the measured cycle and the simulated cycle.

Efficiency and fuel consumption improvement can be reached when it becomes possible to decrease the minimum line pressure (for example Variant C and Variant D from table 1). Decreasing the line pressure will increase the risk of slip. As mentioned before, road irregularities may cause short torque peaks in the drive train, causing a temporary macro-slip condition. The implemented slip controller should avoid these problems. Interesting is the question in which way the control strategy S_f = 1.3 can handle with such torque peaks.

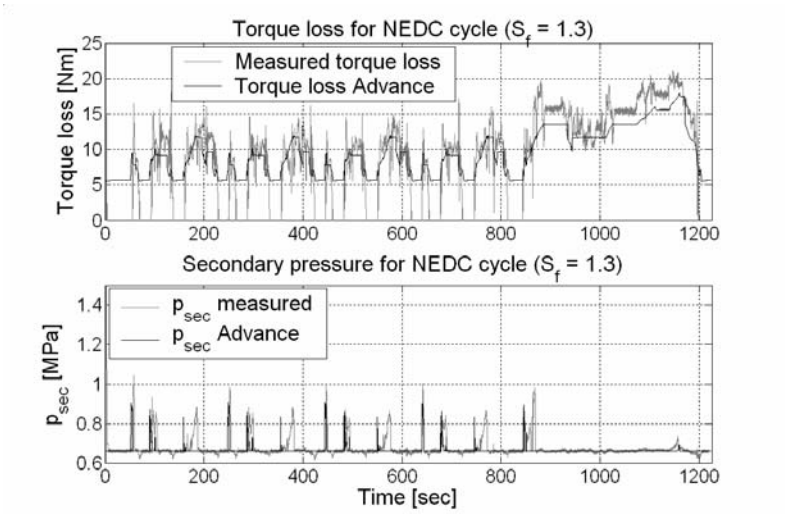

Figure 14: Torque loss and secondary pressure

In Fig. 15 a simulation is shown with the reference CVT with a minimum line pressure of 6.6 [bar] (Variant B) in comparison with a CVT with minimum line pressure of 1.35 [bar] (Variant D), both slip controlled. These results show that the CVT with decreased minimum line pressure has lower torque losses, while the amount of slip is within acceptable limits. So when the line pressure can be decreased, the efficiency will increase and the fuel consumption will decrease. Also the fuel consumption for both cases can be simulated. As expected, the fuel consumption for a CVT with minimum line pressure of 1.35 [bar] (Variant D) will be lower and gives a benefit of approximately 2.2 %. The same simulation can be done for the FTP-72 cycle. For this cycle the CVT with decreased minimal pressure gives a profit of around 1.5 %.

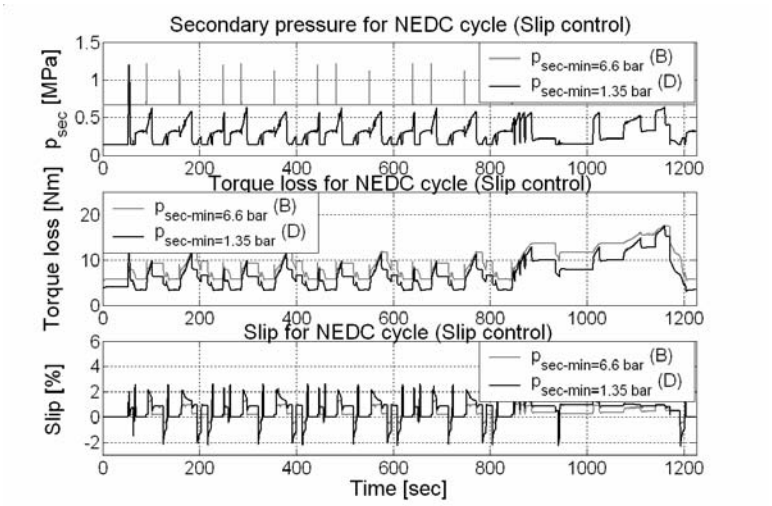

Figure 15: Secondary pressure, torque loss and slip for the reference CVT (B) and the CVT with decreased minimal pressure (D)

In Fig. 16 the comparison has been made between a CVT with decreased minimum line pressure p_{sec_min} = 1.35 [bar] (D) and the EMPAct system (E). The secondary clamping forces resulting from the measurements are almost equal. The advantage of the EMPAct system is the removal of the oil pump, and therefore the removal of these torque losses. The oil pump always rotates at engine speed and therefore dissipates always an amount of power. The torque losses for the EMPAct system are significantly lower.

Because of the decrease in torque loss for the EMPAct system, the efficiency will increase and therefore the fuel consumption will decrease. In comparison to a CVT with decreased minimum line pressure of 1.35 [bar] (Variant D), the new EMPAct system (Variant E) has an advantage of almost 4 percent for the NEDC cycle.

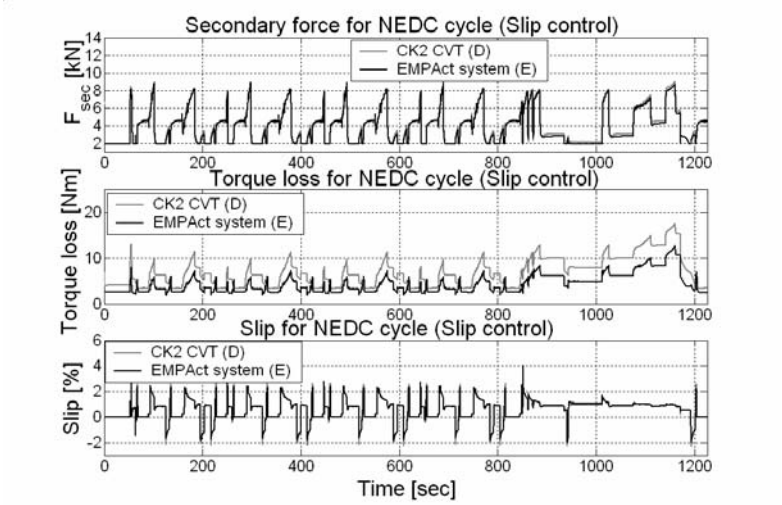

Figure 16: Secondary clamping force, torque loss and slip for the CVT with decreased minimal pressure (D) and the EMPAct system (E)

When the EMPAct system (E) is compared to the conventional CVT (Variant A) an advantage of 6 percent can be reached, see Fig. 17. For the FTP-72 cycle the same simulations can be made. Also here the EMPAct system (E) results in lower torque losses and slip can be kept within acceptable limits. For the FTP-72 cycle the EMPAct system (E) has a fuel consumption benefit of 4.2 percent compared to the CVT

with decreased line pressure (D). In comparison with the conventional CVT (A), the EMPAct system (E) has a benefit of around 5.7 % with respect to fuel consumption.

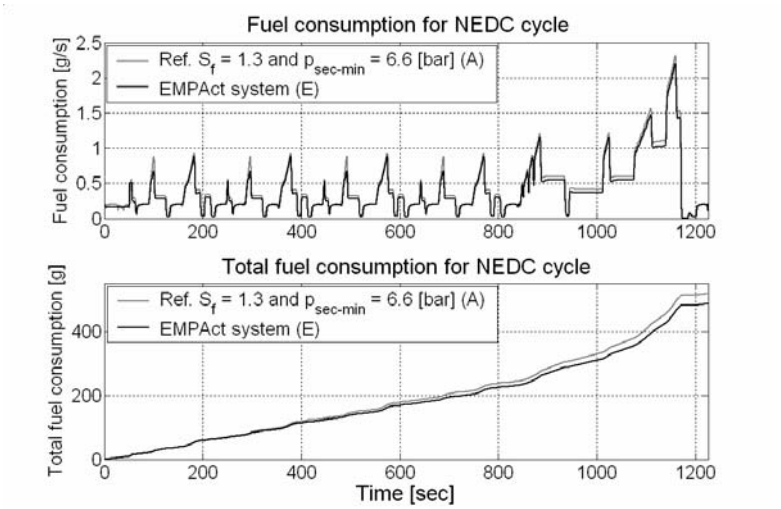

Figure 17: Fuel consumption for Variant A and Variant E during the NEDC cycle.

The results for the two different speed cycles are summarized in the table 2.

Table 2: Fuel consumption reduction for different clamping force control strategies

Clamping force control strategy		Fuel consumption reduction [%]	
Reference:	Compared to:	NEDC	FTP-72
Safety strategy 1.3 (A)	Slip controller (B)	0	0
Slip controller (B)	Slip controller with minimum pressure (D)	2.2	1.5
Slip controller with minimum pressure (D)	EMPAct (E)	4	4.2
Safety strategy 1.3 (A)	EMPAct (E)	6	5.7

10 Conclusions and recommendations

Both model calculations and test rig measurements have been used to construct a detailed efficiency model of a commercially available CVT. The model results are compared to the measurements results and show similarity to these results. By subtracting pump loss and adding loss due to the EMPAct system and by mapping variator loss as a function of over-clamping, the effect of the new actuation system and slip control on the efficiency can be estimated and an indication is given for the consequences for fuel consumption. By applying a servo-electromechanical actuation system and variator slip control, significant reduction of power loss can be expected. This leads to a large improvement of efficiency, especially at part load, which in turn leads to a significant fuel economy potential, especially on driving cycles where part load conditions prevail (about 6% on the NEDC cycle). Simulations for fuel consumption reduction are made with the simulation package Advance, developed by TNO Netherlands.

The proposed servo-electromechanical actuation system is currently in the realization phase. The slip control technique will be optimized, but it has already been applied and demonstrated in a passenger car.

References

[1] K.G.O. van de Meerakker, P.C.J.N. Rosielle, B. Bonsen, T.W.G.L. Klaassen, N.J.J. Liebrand, Mechanism proposed for Ratio and Clamping Force Control in a CVT, in Fisita 2004; Barcelona, Spain, pp. 10, (2204).

[2] Faust, H., M. Homm, M. Reuschel, ”Efficiency-Optimized CVT Hydraulic and Clamping System”, proceedings International CVT congress, VDI berichte 1709, pp.43-58, Munich, Germany, 2002.

[3] Bradley, T.H. and A.A. Frank,”Servo-pump hydraulic control system performance and evaluation for CVT pressure and ratio control”, proceedings International CVT congress, VDI berichte 1709, pp.35-41, Munich, Germany, 2002.

[4] Abo, K., M. Kobayashi, M. Kurosawa, “Development of a metal belt-drive CVT incorporating a torque converter for use with 2-liter class engines”, SAE Technical Paper 980823, 1998.

[5] Changenet, C., M. Pasquier, “Power losses and heat exchange in reduction gears: numerical and experimental results”, International conference on gears, Munich, 2002. VDI berichte 1665.

[6] Bonsen, B., T.W.G.L. Klaassen, K.G.O. van de Meerakker, M. Steinbuch and P.A. Veenhuizen, ”Analysis of slip in a continuously variable transmission”, Proceedings of IMECE03 2003 ASME International Mechanical Engineering Congress, Washington, D.C., November 1521, 2003, IMECE 2003-41360.

[7] Ide, T., ”Effect of Power Losses of Metal V-belt CVT Components on the Fuel Economy”, Proceedings of the International Congress on Continuously Variable Transmission, CVT ’99, Eindhoven, the Netherlands, 1999.

[8] Bonsen, B., T.W.G.L. Klaassen, K.G.O. van de Meerakker, P.A. Veenhuizen and M. Steinbuch, “Measurements and control of slip in a continuously variable transmission”, in Mechatronics 2004, Sydney, Australia 2004.

[9] Drogen, M. van, M. van der Laan, ”Determination of Variator Robustness under Macro Slip Conditions for a Push Belt CVT”, SAE Technical paper, 2004-01-0480, SAE world Congress, Detroit, 2003.

[10] Akehurst, S, “An investigation into the loss mechanisms associated with a pushing metal V-belt continuously variable transmission”, PhD-thesis University of Bath 2001.

[11] Klaassen T.W.G.L., B.G. Vroemen, B. Bonsen, K.G.O. van de Meerakker, M. Steinbuch and P.A. Veenhuizen, “Modeling and simulation of an electro-mechanically actuated push belt type continuously variable transmission”, 3rd IFAC Symposium on Mechatronic Systems, Australia, 2004.

[12] Vink, W., J. Eelkema, J. Zuurbuur, “Modular vehicle simulation in Matlab/ Simulink”, Versuch, Test und Simulation in Antriebsstrang und Fahrwerk Conference, Karlsruhe, Germany, 2002.

[13] Veenhuizen, P.A., B. Bonsen, T.W.G.L. Klaassen, K.G.O. van de Meerakker, M. Steinbuch and F.E. Feldpaus, “Simulated behavior of a vehicle with V-belt type geared neutral transmission with variator slip control, the Netherlands.

[14] Pulles R.J., B. Bonsen, M. Steinbuch and P.A. Veenhuizen, “Slip controller design and implementation in a Continuously Variable Transmisión”, American Control Conference, Portland, Oregon, United States, 2005.

Attachements

This chapter gives recommendations which are not important enough to mention in the paper, but can be used for future work. Also an explanation of the next appendices is given.

A Recommendations and Appendices

The modeling of the CK2 CVT in Matlab (chapter 3) seems be done in a correct way. For all components of the CVT models of loss contributions are implemented, only for the torque converter a model is missing. When the model will be used for situations with an open torque converter, also a model of the torque converter should be implemented.

In Advance the simulations can be made which can be compared to the measurements. The simulation in Advance runs at low speed when the wrong solver is chosen (chapter 9). It is therefore important to choose the correct solver (ode23tb(stiff/TR-BDF2)) and the correct initial step size and relative tolerance. Interesting is to find out if it is possible to use other solvers by adapting the model in the simulation.

To be sure of the results simulated with Advance for the EMPAct system (chapter 8), the results should be compared to the measurements when the EMPAct system is operational on the test rig.

The information given in Appendix B – Appendix G is included in this report to give some more details about subjects treated in the paper. In Appendix B a cross-section of the Jatco CK2 CVT is shown, while in Appendix C the torque loss definition is given which will also be used in Appendix D, the Matlab model. This Matlab model is compared to simulations resulting from the simulation package Advance, which is described in Appendix E. In Appendix F the structural representation of the CK2 model is shown which is used in Advance. Finally, in Appendix G the modeling of the EMPAct system is mentioned.

B Cross-section of the Jatco CK2 CVT

Fig. B.1. shows the cross-section and important part names of the Jatco CK2 CVT, which is used in this research program. For a complete and detailed description of the CK2 and its components the reader is referred to [7].

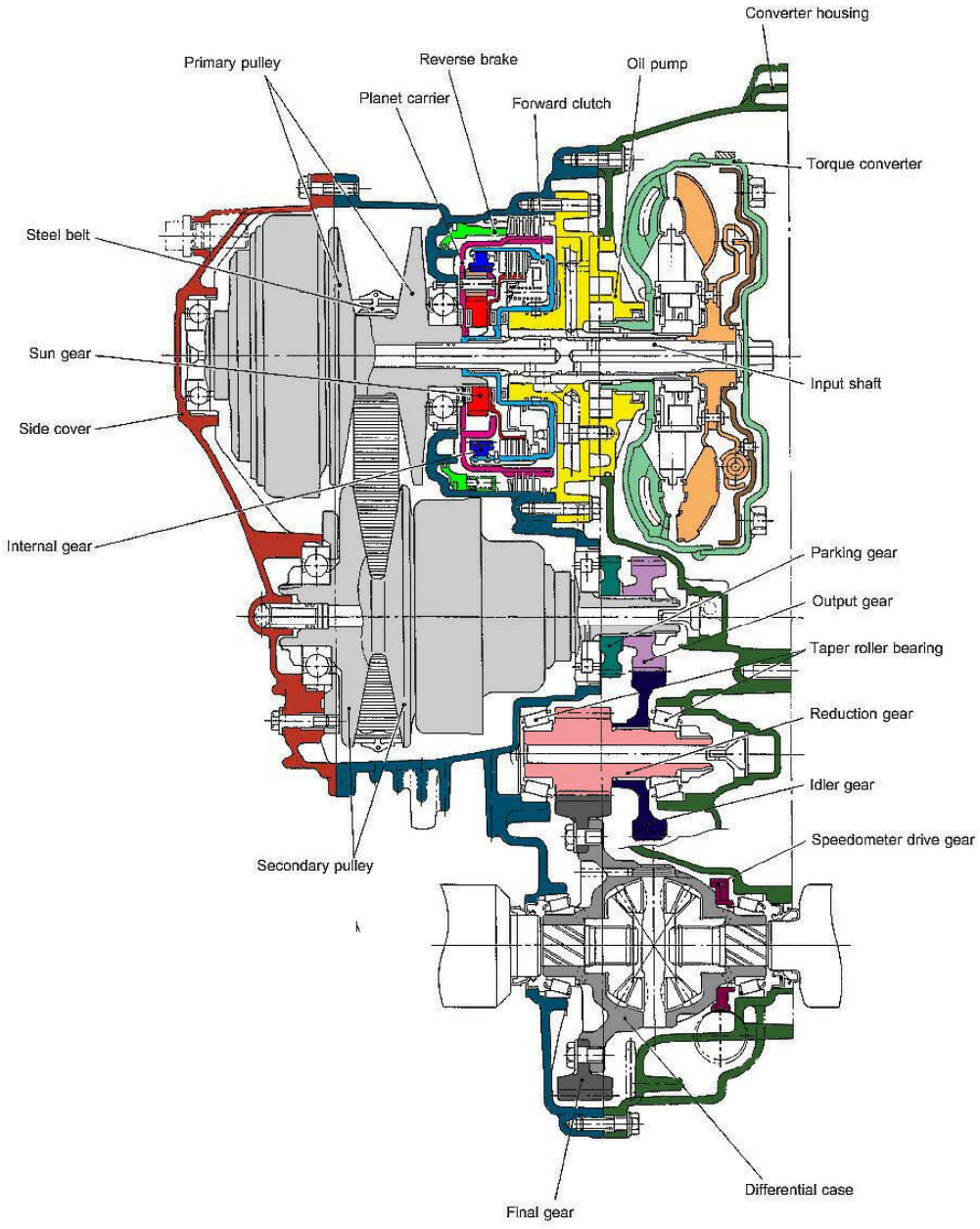

Figure B.1: Cross-section of the Jatco CK2

C Torque loss definition

Before making a Matlab model of the Jatco CK2 CVT (Chapter 3 and Appendix D) first the definition of torque losses will be explained. The torque losses can be calculated with the Eq. C.1 [13].

$$T_{loss} = T_{pri} - r_{T0} T_{\sec} \tag{C.1}$$

where:

T_{pri} = the primary torque of the variator

r_{T0} = the torque ratio at zero load

T_{sec} = the secondary torque of the variator

From earlier experiments [13] it becomes clear that the torque ratio at zero load r_{T0} is equal to the geometric ratio r_G and to the speed ratio at zero load $r_{\omega 0}$. So this means:

$$r_{T0} = r_G = r_{\omega 0} \tag{C.2}$$

Due to the slip also a speed loss will be present. This speed loss can be calculated with Eq. C.3.

$$\omega_{loss} = \omega_{pri} - \frac{\omega_{\sec}}{r_{\omega 0}} \tag{C.3}$$

Slip s_ω can be defined with the following equation:

$$s_\omega = 1 - \frac{r_\omega}{r_{\omega 0}} \tag{C.4}$$

where the speed ratio r_ω can be defined as:

$$r_\omega = \frac{\omega_{\sec}}{\omega_{pri}} \tag{C.5}$$

With Eq. C.2 and Eq. C.4 it is possible to transform Eq. C.1 in Eq. C.6.

$$T_{loss} = T_{pri} - \frac{r_\omega}{1 - s_\omega} T_{\sec} \tag{C.6}$$

The same transformation can be made for Eq. C.3. Combining this equation with Eq. C.4 gives a new expression for the slip losses. These slip losses can now be calculated with:

$$\omega_{loss} = \omega_{pri} - \frac{\omega_{\sec}}{r_\omega}\left(1 - s_\omega\right) \tag{C.7}$$

To translate both losses to power losses first Eq. C.1 and Eq. C.3 have to be transformed. For T_{sec} and ω_{sec} the following equations can be found:

$$T_{\sec} = \frac{T_{pri} - T_{\sec}}{r_{T0}} \tag{C.8}$$

and

$$\omega_{\sec} = \left(\omega_{pri} - \omega_{loss}\right) r_{\omega 0} \tag{C.9}$$

Now the power on the output shaft of the CVT variator can be calculated. In this equation r_{T0} and $r_{\omega 0}$ have the same value and so dividing these parameters gives value 1.

$$P_{\sec} = T_{\sec}\omega_{\sec} = \frac{T_{pri} - T_{loss}}{r_{T0}}\left(\omega_{pri} - \omega_{loss}\right) r_{\omega 0} = \left(T_{pri} - T_{loss}\right)\left(\omega_{pri} - \omega_{loss}\right) \tag{C.10}$$

When the last part of Eq. C.10 was multiplied the following equation for P_{sec} can be found:

$$P_{\sec} = T_{pri}\omega_{pri} - T_{loss}\omega_{pri} - \omega_{loss}T_{pri} + \omega_{loss}T_{loss} \tag{C.11}$$

Rewriting Eq. C.11 gives the following expression for the power losses due to torque loss and speed loss:

$$P_{pri} - P_{\sec} = P_{torque-loss} + P_{slip-loss} - P_{remaining} \tag{C.12}$$

where the last term $P_{remaining}$ can be neglected because of its small size.

D Matlab model

This Matlab model is validated with measurements from the test rig and the data mapped in lookup tables is implemented in Advance. Before running the model first an engine speed ω_{eng} should be defined. This speed can vary between 500 and 2500 [rpm]. Then a column of torques is generated where the maximum torque is 200 Nm. This 200 Nm is the maximum torque the CK2 CVT can handle. Also a column of geometric ratios is generated where the ratio varies between 0.43 and 2.2. These two borders are the low and OD ratio of the CK2 CVT. Now the different functions will be given which are used in the CVT model.

D.1 Function r2Rp

The function r2Rp calculates the running radius of the primary pulley R_{pri}. This radius can be obtained using Eq. D.1:

$$L = 2CD\cos(\lambda) + R_{pri}(\pi + 2\lambda) + R_{\sec}(\pi - 2\lambda) \tag{D.1}$$

where:

L	= Circumferential length of the belt
CD	= Pulley center distance
λ	= Pulley wedge angle
R_{pri}	= Running radius of the belt on the primary pulley
R_{sec}	= Running radius of the belt on the secondary pulley

Together with the equation for the geometric ratio r_G it is possible to transfer Eq. D.1 to an ABC-formula with only an unknown parameter R_{pri}. For this equation the circumferential length of the belt and the pulley center distance should be known.

D.2 Function F_{clamp}

Function file F_{clamp} calculates the minimum clamping force on the secondary pulley. In Eq. D.2 the really desired clamping force F_{sec} is given:

$$F_{\sec} = F_{pri} + F_s + F_c \tag{D.2}$$

where:

F_{pri}	Clamping force on the primary pulley
F_s	Spring force
F_c	Centrifugal force

Next a safety strategy S_f has to be chosen so the clamping force on the secondary pulley can be determined. S_f determines the clamping force on the secondary pulley.

D.3 Function s_ω

In the function file s_ω the slip acting on the belt can be calculated. In figure D.1 a traction curve is shown of a measurement of slip versus the friction coefficient μ. The derivative of the linear part near to zero is

called α. From many experiments all different values for α are found which depends on clamping force and geometric ratio. For three different ratios (low, medium and OD ratio) and variable secondary clamping forces (F_{sec}) the measurement data has been plotted in Fig. D.2.

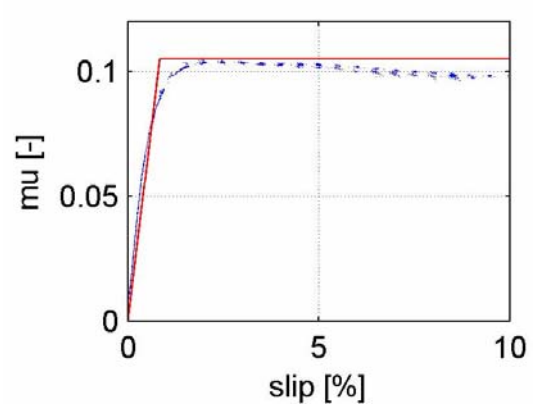

Figure D.1: Slip percentage versus μ

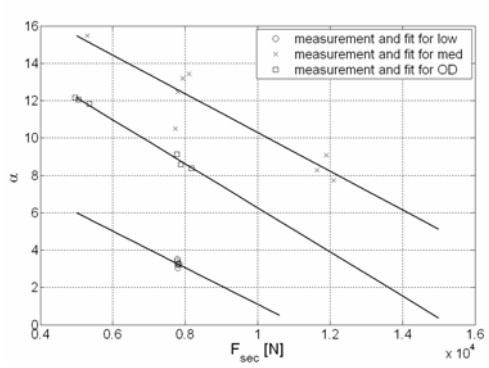

Figure D.2: Fit through data of measurements

Through this measured data a first order polynomial fit has been plotted. This polynomial fit gives a relation between the secondary clamping force F_{sec} and the value of α given by Eq. D.3.

$$\alpha = -0.001\left(F_{\text{sec}} - F_c\right) + \alpha_{\text{int}} \tag{D.3}$$

where:

F_{sec} = Clamping force on the secondary pulley

F_c = Constant clamping force on the secondary pulley

α_{int} = Interpolated value of α for different ratios

At the level of F_c (about 7.8 kN) three nearly constant values for α were measured. For high axial forces three different constant values for α were found. The minimum value of α belongs to the constant α for high axial forces. This protects α to become never too small or even negative. By interpolating the real geometric ratio over the measured values for low, medium and OD you can find an estimated value for the acting α_{int}. Together with α it is possible to determine an interpolated value for the slip s_ω. In Eq. D.4 the definition of slip is given.

$$s_\omega = \frac{\mu_{eff}}{\alpha} \tag{D.4}$$

Normally the slip value s_ω will be around the 1 %.

D.4 Function T_{pump}, T_{var}

To calculate the oil pump and variator torque losses the lookup tables described in chapter 3 has been used. The pump losses depend on the engine speed, secondary pressure and oil temperature, while the variator losses depend on the primary pulley speed, geometric ratio and secondary pressure.

D.5 Function FR_{loss}

Function file FR_{loss} determines the final reduction torque losses. The final reduction consists of four gears which will decrease the speed and increase the torque. The final reduction losses depend on the ingoing speed, the ingoing torque and the oil temperature. The power losses can be divided into tooth friction losses, bearing losses and oil churning losses.

In this function file first the parameters of the gears should be noted. When all the parameters are given the function file for the oil churning losses can be loaded. These oil churning losses depends on the ingoing torque of the gear, gear parameters and oil properties. Next the tooth friction losses can be determined. These losses due to tooth friction depends on the gear parameters, ingoing torque of the driven gear and the oil properties. The results of this function file are the axial and radial force acting in the tooth contact and of course the tooth friction power losses. For the second set of gears the same can be done. The third losses in the final reduction are the losses of the bearings. Also for these losses a function file has been written. This function file depends on the different axial and radial forces acting in the tooth contact points and on the different speed of gears. When the bearing losses are add to the oil churning losses and the tooth friction the total final reduction power losses are known and therefore the efficiency of the whole final reduction.

$$P_{FR-out} = P_{FR-in} - P_{FR-loss} \tag{D.5}$$

E Advance

In Advance the user is able to perform a wide range of different vehicle simulations. The modular setup of the toolbox opens the possibility for the user to combine Advance with models of vehicle subsystems developed outside Advance in user-defined libraries. In Advance different modules have been created that represent specific areas of the simulation of vehicle dynamics. The user sees these different areas represented by subsystems in the Simulink basic vehicle model layout. When working with Advance the user can create efficient models that are tailor-made for the behavior that is investigated. Advance has been built in MATLAB/Simulink. The calculations that are performed in each standard module have been transformed into efficient s-functions to improve the speed of the simulations. Advance is developed so that it can be used for real-time applications.

Advance models are divided into the following levels:

Top level
This is the uppermost level of the model, representing the complete vehicle. This level appears when a new model is created.

Areas
The areas, located in the top level of the model, represent the various vehicle subsystems, such as power train and chassis. While they have no built-in functionality, they are used to define the model structure. Areas can contain Advance modules, standard Simulink sub-systems and blocks.

Modules
Modules simulate the behavior of each of the vehicle components. These include e.g. the body, engine and wheel kinematics modules. The available modules are present in the Advance library in the Simulink Library Browser. Modules need to be placed in areas or lower in the vehicle structure.

Top level of an Advance model

The top level of the model structure shows six areas that contain all the vehicle modules that are used (see Fig. E.1). The model handling, the setting of the parameter files, viewing the time traces and selecting the output functions are all placed on the top level of the model layout in the green areas. The collection of the data that comes out of the model areas is part of the data bus that is used in Advance. The data bus is used to enable data access in all model levels.

The six main vehicle areas are gray. They represent six important aspects of the modeling of the vehicle dynamics. The areas don't have any direct functionality. However, by using them the Simulink model will always have a similar organization and the fixed structure will support the intuitive use of the model. Specialized graphical user interfaces support the user when performing the simulations.

The following vehicle areas have been defined:

test
In this area a predefined vehicle test can be placed. Such a test can be e.g. a step steer test or a power train load cycle test (for example the NEDC or FTP-72 cycle).

driver
In this area the used driver model can be placed. In the first release of Advance driver models will be part of the library.

control
This area contains the vehicle controllers that are used to control vehicle dynamics and power trains. These units are i.e. gear and throttle control for automatic vehicles and traction control systems.

power train
The power train area is created for all power train components.

chassis
In Advance the chassis is defined as the part of the vehicle containing the tires, wheels and suspension.

body
Different models for the main body of the vehicle.

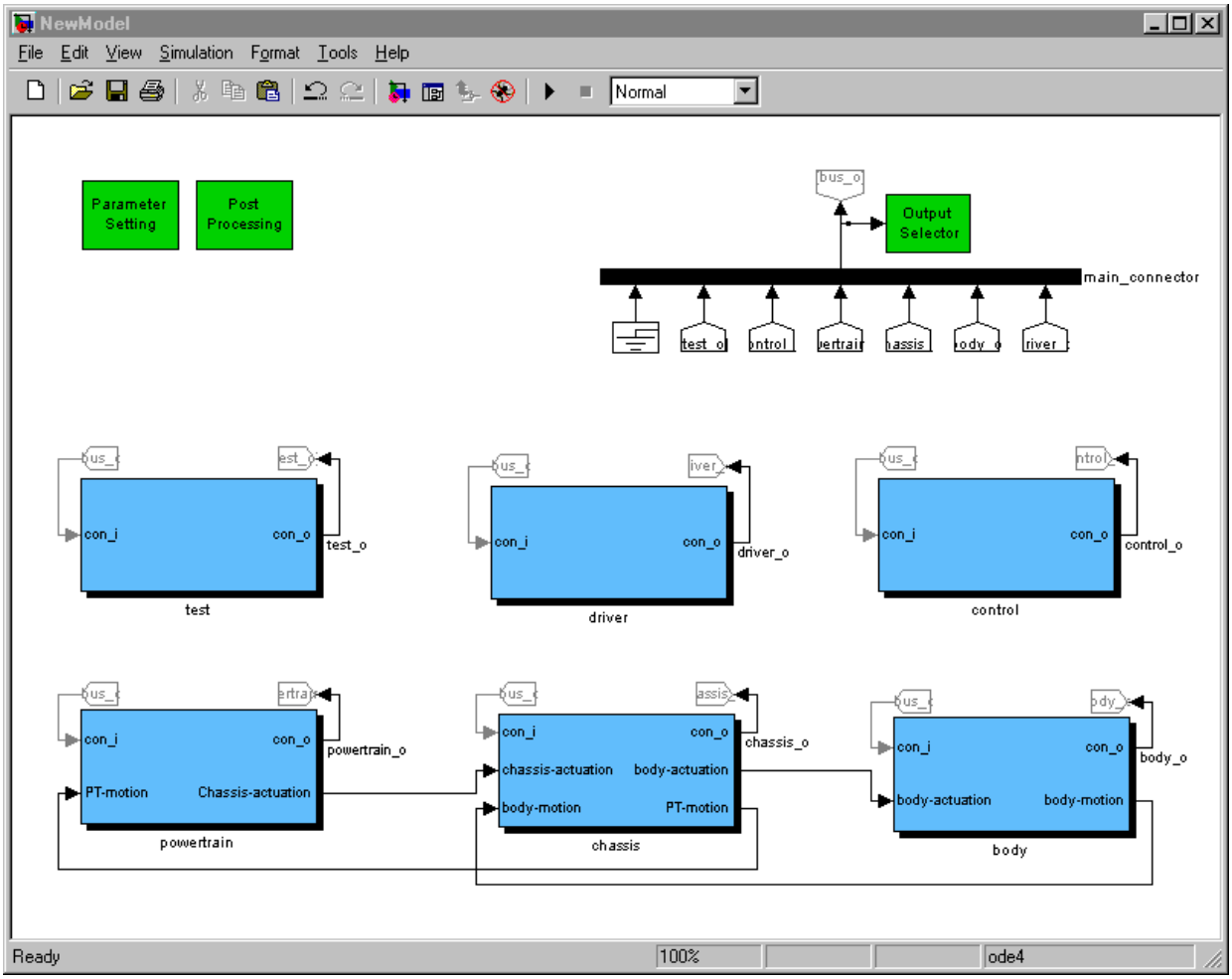

Figure E.1: The top level of the model structure

F Modeling the CK2 in Advance

For modeling the CK2 in Advance an adapted model of R. Pulles has been used [14]. The model is created in Advance using existing variator models that describe shifting behavior, torque transmission, and belt slip. Additionally, the measured torque losses caused by the oil pump and the variator are incorporated in the model using look-up tables. And finally, the line pressure circuit and the ratio control circuit were modeled to complete the model. The structure of the total model is shown in Fig. F.1.

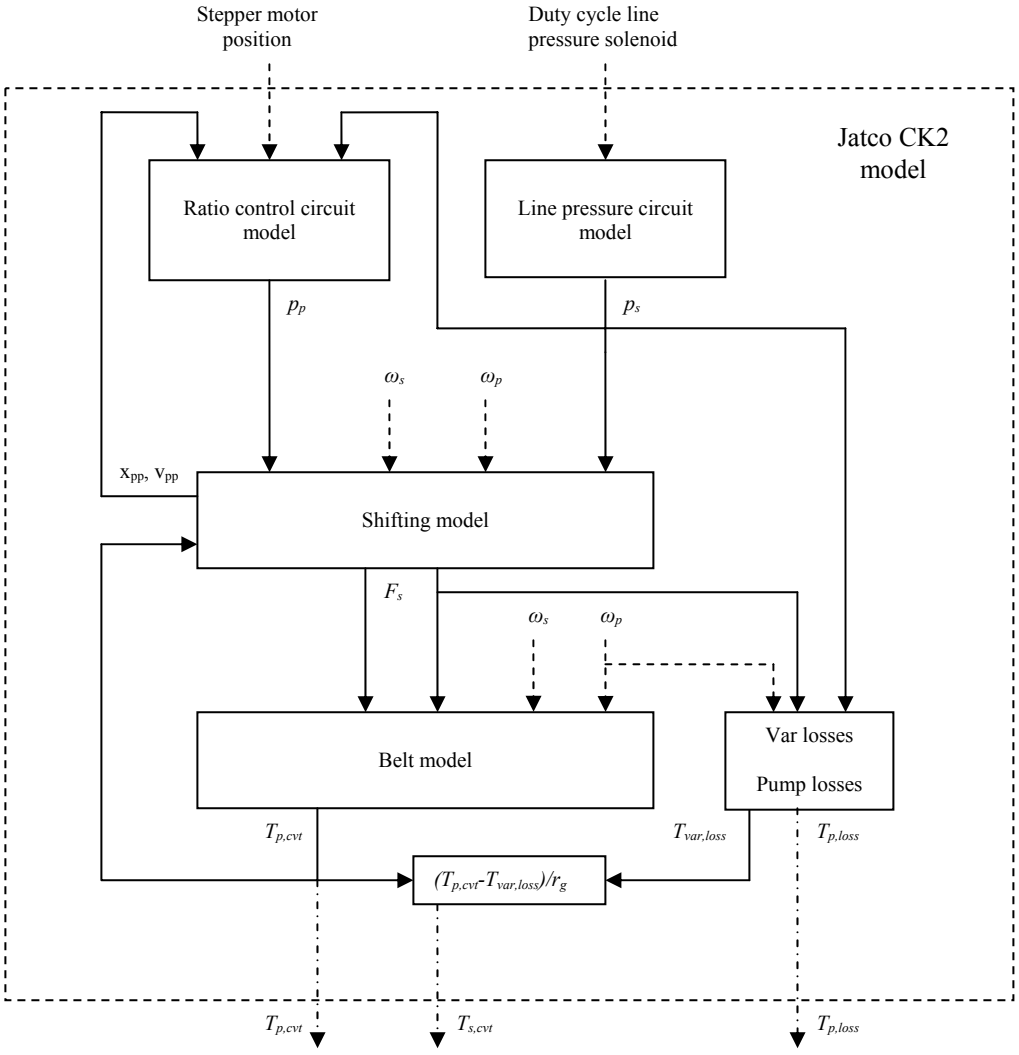

Figure F.1: Structural representation of the CK2 model in Advance

In this figure the stepper motor position results from the ratio controller. Here the speed ratio is controlled to the reference ratio resulting from the variogram. For safety strategy 1.3 the duty cycle line pressure solenoid is calculated with Eq. 3 in chapter 3. Here the secondary clamping force is multiplied with a factor 1.3. For the slip controller the duty cycle line pressure solenoid is calculated with the same equation only with safety factor 1. This part is calculated as feed forward for the duty cycle. The total duty cycle is completed with a value calculated from the difference between slip and slip set point.

G Modeling the EMPAct system in Advance

For the EMPAct system a little model has been written which predicts the torque losses due to tooth friction losses in the planetary gear sets. This is because the simulations described in chapter 8 were not done in time for the deadline of the paper.

The model calculates from the different torques on the primary and secondary shaft the primary and secondary clamping force respectively. Together with the speed belonging to both shafts the sliding speed can be calculated. Multiplying the clamping force with the sliding speed the power of tooth contact is calculated. For each shaft there are four contacts and for each contact an efficiency of 99% has been taken. Adding all the power losses gives an amount for the power loss due to the tooth friction contact in the planetary gear sets.

Also for the oil pump for auxiliaries and for the electric motors in Fig. 7 and amount of power is absorbed too. All this power is all subtracted from the input power on the primary shaft and the remaining power is available on the secondary shaft.

Nomenclature & Acronyms

ACRONYMS

Symbol	Description
CVT	Continuously Variable Transmission
NEDC	New European Driving Cycle
FTP-72	Federal Test Procedure
EMPAct	Servo-electromechanical actuation system

SYMBOLS

Symbols	Description	[Unit]
CD	Pulley center distance	[m]
A_{sec}	Secondary cylinder piston area	[m^2]
F_{pri}	Primary pulley clamping force	[N]
F_{sec}	Secondary pulley clamping force	[N]
F_c	Centrifugal force	[N]
F_s	Spring force	[N]
L	Length of V-type belt	[m]
p_{sec}	Secondary pressure of hydraulic oil	[Pa]
$p_{sec\text{-}min}$	Minimum secondary pressure of hydraulic oil	[Pa]
P_{pri}	Power on the primary shaft	[W]
P_{sec}	Power on the secondary pulley	[W]
$P_{slip\text{-}loss}$	Power loss due to slip	[W]
$P_{torque\ loss}$	Power loss due to transferring torque	[W]
$P_{remaining}$	Remaining term for power loss	[W]
R_p	Primary pulley running radius	[m]
r_G	Geometrical ratio	[-]
r_ω	Rotational speed ratio	[-]
$r_{\omega 0}$	Zero load speed ratio	[-]
r_{To}	Torque ratio at zero load	[-]
S_f	Safety factor	[-]
s_ω	Relative slip number	[-]
T_{pri}	Primary shaft torque	[Nm]
T_{sec}	Secondary shaft torque	[Nm]
T_{loss}	Torque loss measured at primary side	[Nm]
α	Derivative of linear part of a traction curve	[-]
λ	Pulley wedge angle	[rad]
μ	Friction coefficient of V-belt type belt and pulley sheave contact	[-]
μ_{eff}	Effective friction coefficient	[-]
ω_{loss}	Variator slip loss	[rad/s]
ω_{pri}	Rotational speed primary intermediate shaft	[rad/s]
ω_{sec}	Rotational speed secondary intermediate shaft	[rad/s]

Table of figures

Table of tables

Samenvatting

Moderne controle technieken maken het mogelijk om aandrijfcomponenten van voertuigen onder meer optimale condities te laten opereren dan voorheen. Krachtige electrische servo-motoren en moderne controllers zijn noodzakelijk voor de ontwikkeling en verfijning van automatische transmissies zoals de Double Clutch Transmissie en de Continu Variabele Transmissie. Dit alles om het brandstof verbruik, comfort en performance niveau te bereiken wat verwacht kan worden van huidige voertuigaandrijvingen.

Om aan te tonen wat het effect is van de verschillende verbeteringen met betrekking tot het brandstofverbruik kunnen in het begin van het ontwikkelings proces gedetailleerde simulaties gemaakt worden welke gebasseerd zijn op de bovenstaande technologie. Dit paper beschrijft het resultaat van een simulatie studie naar de effecten op gebied van efficientie en het brandstofverbruik in een voertuig uitgerust met een CVT, wat resulteert uit de introductie van het volgende nieuwe actuatie systeem en controle technieken [1]:

- Vervanging van de hydraulische hoge druk pomp door een servo-electromechanisch actuatie systeem (EMPAct) en
- Introductie van variator slip controle

Voor deze studie is het simulatie pakket Advance van TNO gebruikt. In dit pakket zijn gedetailleerde modellen van alle verliesbijdragende componenten van de CVT geimplementeerd. De winst in brandstofverbruik is substantieel, ongeveer 6% op de NEDC cyclus.

Acknowledgment

I would like to thank my coach Bram Veenhuizen for his support and guidance during the project. Also I want to thank Tim Klaassen for his support during my final project, especially for his help on the test rig. Special thanks go out to all students in the student's room in general and to Rob Pulles in special for all his help on the test rig and modeling.

Finally I want to thank my family and my girlfriend in special for all their support during my final study.